

THERMOELASTIC DAMPING IN FLEXURAL-MODE RING GYROSCOPES

Zhili Hao

School of Electrical and Computer Engineering
Georgia Institute of Technology
777 Atlantic Drive, Atlanta GA 30332-0250 USA
zhili.hao@ece.gatech.edu

Farrokh Ayazi

School of Electrical and Computer Engineering
Georgia Institute of Technology
777 Atlantic Drive, Atlanta GA 30332-0250 USA
farrokh.ayazi@ece.gatech.edu

ABSTRACT

This paper provides a comprehensive derivation for thermoelastic damping (TED) in flexural-mode ring gyroscopes, in light of recent efforts to design high rate-resolution gyroscopes. Imposing an upper limit on the attainable mechanical noise floor of a vibratory gyroscope, thermoelastic damping in a ring gyroscope is extracted from the equations of linear thermoelasticity. By assuming that it is small and therefore has negligible effect on the flexural-mode vibrations in a ring, thermoelastic damping manifests itself through temporal attenuation, where a complex frequency is used to quantitatively evaluate this damping. The exact solution to thermoelastic damping is derived and verified with experimental data in the literature. This work not only provides significant insight to the geometrical design in high-Q ring gyroscopes, but also defines their performance limit.

INTRODUCTION

Micromechanical flexural-mode ring vibratory gyroscopes are of great interest for sensing rotation rate, due to their inherent symmetric structures and better temperature sensitivity [1-4]. One key determinant of performance for a vibratory gyroscope is its mechanical quality factor (Q). Since a higher Q in a gyroscope translates to higher rate-resolution, better bias stability, and lower power consumption, the design of a ring gyroscope with high Q or little energy loss is consistently pursued. Identified as a fundamental loss mechanism, thermoelastic damping (TED) imposes an upper limit on the attainable Q and further determines mechanical noise floor ($\Omega_{\text{mechanical}}$) of a ring gyroscope. Thus, it is of significant importance to understand thermoelastic damping in ring gyroscopes, not only for improving their performance, but also for establishing their performance limit.

Although the physical mechanism and theory of thermoelasticity has been well established [5], analytical studies on thermoelastic damping in flexural-mode vibrations of different finite-geometries are few. In the 1930's, by introducing the resonant mode shapes into the equation of heat conduction and obtaining the corresponding transverse thermal modes, Zener derived an approximate expression for thermoelastic damping in rectangular beams undergoing flexural-mode vibrations [6,7]. Through keeping the first transverse thermal mode and neglecting the rest thermal modes, Zener's theory showed that thermoelastic damping in a flexural beam exhibits a Lorentzian behavior with a single thermal relaxation time. This relaxation time is related to the width b of the beam and the thermal diffusivity χ of the material used. Without neglecting any transverse thermal modes, Lifshitz and Rouke's recent work [8] provided an exact solution to the linear thermoelastic equations in flexural-mode beam resonators, predicting a modified Lorentzian behavior of the thermoelastic damping.

Both the above-mentioned works have a fundamental assumption that thermoelastic coupling is very weak and thus has negligible influence on the uncoupled elastic resonant modes of a beam, so the elastic and thermal problems are essentially decoupled. This assumption is necessary, since severe thermoelastic coupling would cause noticeable influence on the uncoupled elastic behavior and lead to third-order phenomenon, where quality factor does not exist. Following this assumption, the uncoupled resonant mode shapes are further assumed, in order to find the temperature variation in the beam. Section II will give an overview of thermoelastic damping in a flexural-mode rectangular beam resonator.

In light of recent efforts to design high Q gyroscopes, one particularly interesting aspect of the physical behavior of a ring gyroscope is its thermoelastic damping at different frequencies

and different geometrical design parameters. Recent work has begun to address this issue. For instance, Wong et al. [9] provided a mathematical expression for thermoelastic damping in a ring gyroscope, based on Zener's model for flexural-mode rectangular beams. Their work adopted the thermal relaxation time directly from that of a flexural beam. However, thermoelastic damping in Zener's model was derived from the resonant mode shapes of a rectangular beam for calculating its temperature variation. Since the resonant mode shapes and frequencies of a ring is completely different from those of a rectangular beam, this work falls short of proving a rigorous theoretical derivation and need to be re-examined.

This paper provides a comprehensive derivation of thermoelastic damping in the flexural-mode vibrations of a ring gyroscope to obtain its exact mathematical expression. In order to get a better understanding of the effect of thermoelastic coupling on the flexural-mode vibrations, the thermoelastic-uncoupled governing equations are reviewed, providing mathematical expressions for the uncoupled resonant frequencies and mode shapes. The equations of linear thermoelasticity are then used to evaluate thermoelastic damping. The derived exact solution to thermoelastic damping in a ring gyroscope is further verified with experimental data in the literature. Besides providing significant insight to the geometrical design in high- Q ring gyroscopes, this work defines the performance limit of a ring gyroscope, regarding its attainable mechanical noise floor.

REVIEW OF THERMOELASTIC DAMPING IN FLEXURAL-MODE BEAM RESONATORS

Figure 1 illustrates the thermoelastic damping process in a flexural-mode beam resonator. The laws of thermodynamics predict that variation of strain in a solid is accompanied by a variation of temperature, which causes an irreversible flow of heat. This heat conduction gives rise to an increase in entropy and consequently, to dissipation of vibration energy [5]. This process of energy dissipation is commonly referred to as *thermoelastic damping*.

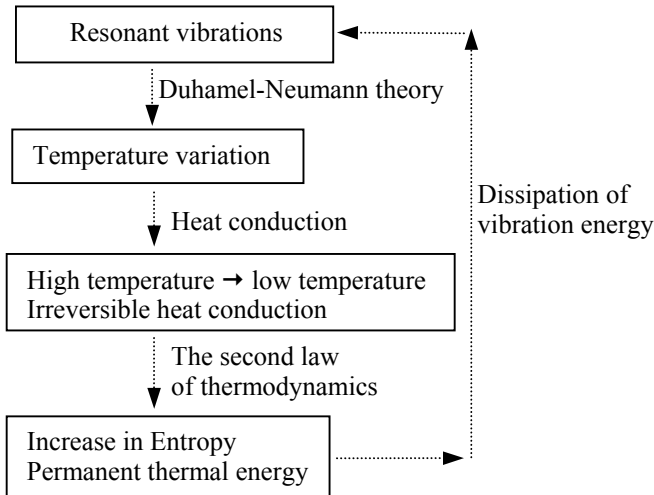


Fig. 1: Thermoelastic damping process in a beam resonator irreversible heat conduction

Zener's model shows that thermoelastic damping behavior in a flexural rectangular beam resonator can be approximately expressed by:

$$Q_z^{-1} = \Delta_E \cdot \frac{\omega \cdot \tau_z}{1 + (\omega \cdot \tau_z)^2} \quad (1)$$

where ω is the angular resonant frequency; Δ_E and τ_z are the thermal relaxation strength and time, respectively, given by:

$$\Delta_E = \frac{E \cdot \alpha_T^2 \cdot T_0}{\rho \cdot C_p} \quad (2)$$

$$\tau_z = \frac{b^2}{\pi^2 \cdot \chi} \quad (3)$$

where, E is the Young's modulus; α_T is the linear thermal expansion coefficient; ρ is the density; C_p is the heat capacitance; χ is the thermal diffusivity of the structural material; and T_0 is the ambient temperature.

In Zener's model, it was assumed that the stress and strain along the beam axis, produced by flexural-mode vibrations of a rectangular beam, vary linearly with the distance from the neutral plane, the one running through the length of the beam suffering no extension or contraction during the vibrations. The other reasonable assumption was that the thermal variation across the beam width is much larger than that along the beam axis, so that only the temperature variation across the beam width is considered for thermoelastic damping. Based on the flexural-mode shapes of a rectangular beam, the transverse thermal modes across the beam width were calculated to evaluate thermoelastic damping quantitatively.

Using the equations of linear thermoelasticity, Lifshitz and Roukes [8] derived an exact solution to thermoelastic damping in a flexural-mode rectangular beam resonator, without an expansion of the transverse thermal modes. In their model, thermoelastic damping manifests itself through temporal attenuation. The effect of thermoelastic damping on the flexural-mode vibrations in a beam is taken into account by the complex frequency expression:

$$\omega = (\omega_r + \omega_i \cdot i) \quad \omega_r, \omega_i \geq 0 \quad (4)$$

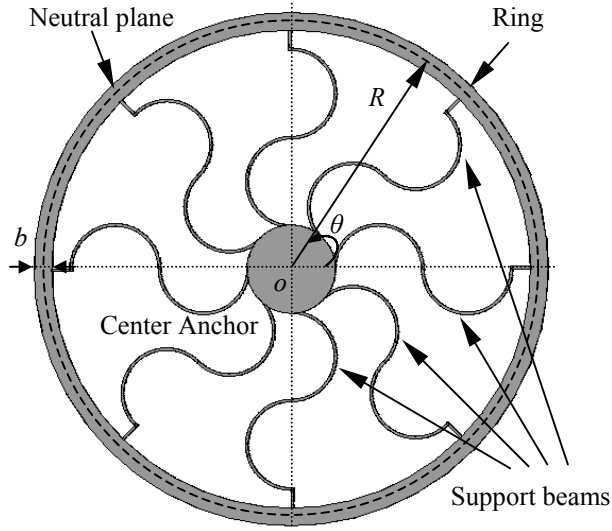
where ω_r is the real value giving the new angular resonant frequency of the beam in the presence of thermoelastic coupling, while ω_i the imaginary value giving the attenuation of the vibrations. The quality factor of thermoelastic damping can be evaluated in terms of the complex frequency [8]:

$$Q_{TED}^{-1} = 2 \cdot \frac{|\text{Im}(\omega)|}{|\text{Re}(\omega)|} \quad (5)$$

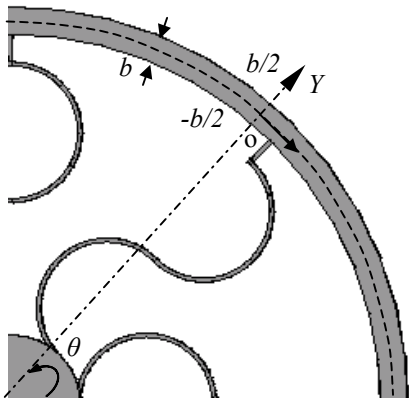
Equation (5) is very general and applicable for evaluating the quality factor in any types of second-order resonators. This work will use this equation to evaluate thermoelastic damping in a ring gyroscope.

FLEXURAL-MODE VIBRATIONS WITHOUT THERMOELASTIC COUPLING

Figure 2(a) illustrates a schematic view of a ring gyroscope, consisting of a ring clamped to the center anchor through eight support beams. In this work, the polar coordinate (r, θ) is used, with origin set at the center of the ring. Generally, by locating electrodes around the outer periphery of the ring, capacitive drive, sense, and tuning mechanisms can be implemented for its operation. This ring is R in radius and has a rectangular cross-section of width b and thickness h . The ring gyroscope experiences the in-plane flexural-mode vibrations involving both radial and circumferential displacements. It is assumed that the support beams have negligible effect on the vibrations of the ring. This assumption is valid as long as the stiffness of the support beams is much smaller than that of the ring [10]. Thus, the ring is modeled as the one with both free inner and outer peripheries (free-edged). For simplicity, it is assumed that the ring gyroscope is made from a linear, isotropic, and homogeneous material.



(a) Ring gyroscope of thickness h



(b) Coordinate along the ring width

Fig. 2: Schematic view of a ring gyroscope

In the absence of thermoelastic coupling, the governing equations for the in-plane flexural-mode vibrations in a ring may be written in the following format [11]:

$$\rho A \cdot \frac{\partial^2 u_\theta}{\partial t^2} = \frac{D}{R^4} \cdot \left(\frac{\partial^2 u_\theta}{\partial \theta^2} - \frac{\partial^3 u_r}{\partial \theta^3} \right) + \frac{K}{R^2} \cdot \left(\frac{\partial^2 u_\theta}{\partial \theta^2} + \frac{\partial u_r}{\partial \theta} \right) \quad (6a)$$

$$\rho A \cdot \frac{\partial^2 u_r}{\partial t^2} = \frac{D}{R^4} \cdot \left(\frac{\partial^3 u_\theta}{\partial \theta^3} - \frac{\partial^4 u_r}{\partial \theta^4} \right) - \frac{K}{R^2} \cdot \left(\frac{\partial u_\theta}{\partial \theta} + u_r \right) \quad (6b)$$

where $D = EI$ and $K = EA$, with E and ρ denoting the Young's modulus and density of the ring structural material, respectively; $I = b^3 \cdot h/12$ is the moment of inertia and $A = b \cdot h$ is the cross-section area.

The displacement vector \bar{u} is defined in terms of the radial (u_r) and circumferential (u_θ) displacements, respectively, expressed as below:

$$\bar{u} = u_r \cdot \bar{r} + u_\theta \cdot \bar{\theta} \quad (7)$$

The solutions to Equations (6) can be expressed as [11]:

$$u_\theta = U_\theta \cdot e^{j\omega_n t} = \frac{-A}{n} \cdot \sin(n\theta) \cdot e^{j\omega_n t} \quad (8a)$$

$$u_r = U_r \cdot e^{j\omega_n t} = A_n \cdot \cos(n\theta) \cdot e^{j\omega_n t} \quad (8b)$$

where ω_n and A_n denote the n th angular resonant frequency and vibration amplitude of the radial displacement, respectively. The flexural mode shapes are expressed in terms of the trigonometric functions. It has been assumed that n , the mode order, is equal to or larger than 2. In this work, we consider only the modes for which $n \geq 2$, as these modes provide degenerate modes for rotation rate sensing. By locating the support beams at the center anchor, the forces from these beams cancel out each other and hence the support loss in the gyroscope is significantly alleviated [12, 13].

As eq.s (8) illustrate, the flexural-mode vibrations in a ring are transverse deflection dominant and the ring is essentially vibrating in bending, analogous to the flexural-mode vibrations of a beam. Experiencing negligible extension and contraction during the vibrations, the neutral plane of the ring is the circular cross-section located at the middle of the ring width, perpendicular to the radial direction, as illustrated in fig. 2(a). Figure 2(b) shows the coordinate for calculating temperature variation across the ring width, where Y -axis starts from the neutral plane of the ring and points toward the radial direction.

Several mode shapes are depicted in fig. 3 to illustrate the in-plane flexural vibration behavior. It should be noted that, for isotropic and homogeneous ring gyroscopes, each flexural-mode is accompanied by its degenerate mode with the same corresponding resonant frequency while $90^\circ/n$ apart in the circumferential direction, in that the cosine and sine functions in u_r and u_θ are exchangeable. It is these two identical degenerate modes that enable rotation rate sensing of a ring.

The n th angular resonant frequency is expressed as [11]:

$$\omega_n^2 = \frac{K_1}{2} \cdot \left(1 - \sqrt{1 - 4 \cdot \frac{K_2}{K_1^2}} \right) \quad (9)$$

where

$$K_1 = \frac{n^2 + 1}{R^2 \rho A} \cdot \left(\frac{n^2 D}{R^2} + K \right) \quad (10a)$$

$$K_2 = \frac{n^2 (n^2 - 1)^2}{R^6 (\rho A)^2} \cdot DK \quad (10b)$$

Generally, the term K_2/K_1^2 is much smaller than unity. Substituting eq.s (10) into eq. (9) leads to the following expression for the n th angular resonant frequency:

$$\omega_n = \frac{1}{\sqrt{12}} \cdot \frac{b}{R^2} \cdot \frac{n(n^2 - 1)}{\sqrt{n^2 + 1}} \cdot \sqrt{\frac{E}{\rho}} \quad (11)$$

where the relation $n^2 D / R^2 \ll K$ has been used.

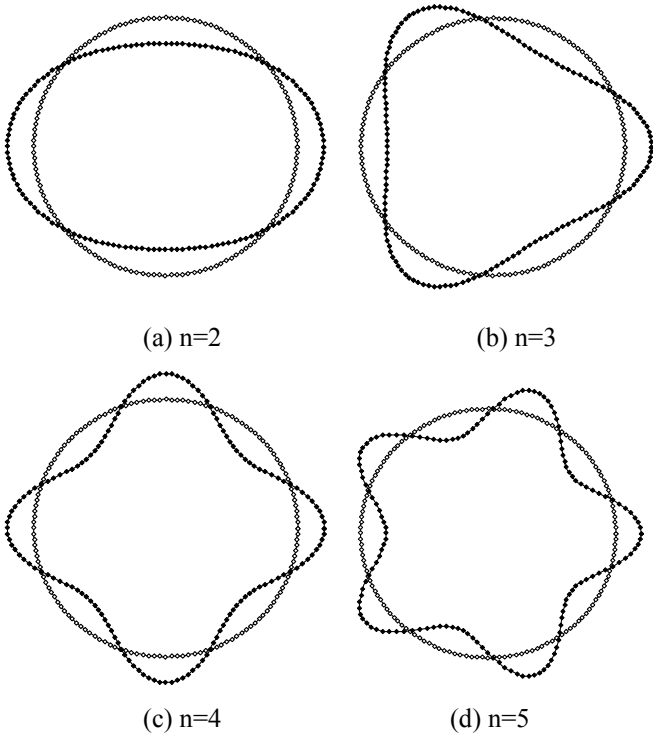


Fig. 3: In-plane flexural-mode shapes in a free-edged ring, with solid triangles symbolizing the vibration modes

FLEXURAL-MODE VIBRATIONS WITH THERMOELASTIC COUPLING

In order to calculate thermoelastic damping in a ring gyroscope, in terms of its geometry and resonant modes, the thermal loads due to the flexural-mode vibrations in the ring need to be introduced into eq.s (6). Because transverse deflection is dominant in the flexural-mode vibrations, it is

assumed that the thermal variation along the circumferential direction is negligible. Thus, thermoelastic damping is solely caused by the temperature variation across the ring width. Since the ring is thin, it is a reasonable assumption that the stress and strain along the ring width vary linearly with the distance (y) from the neutral plane.

Governing equations with thermoelastic coupling

Taking the temperature variation across the ring width into account, the governing equations for the in-plane flexural-mode vibrations are expressed as below [11]:

$$\frac{D}{R^4} \cdot \left(\frac{\partial^2 u_\theta}{\partial \theta^2} - \frac{\partial^3 u_r}{\partial \theta^3} \right) + \frac{K}{R^2} \cdot \left(\frac{\partial^2 u_\theta}{\partial \theta^2} + \frac{\partial u_r}{\partial \theta} \right) \quad (12a)$$

$$- \frac{b}{R} \cdot \frac{\partial N_T}{\partial \theta} - \frac{b}{R^2} \cdot \frac{\partial M_T}{\partial \theta} = \rho A \cdot \frac{\partial^2 u_\theta}{\partial t^2}$$

$$\frac{D}{R^4} \cdot \left(\frac{\partial^3 u_\theta}{\partial \theta^3} - \frac{\partial^4 u_r}{\partial \theta^4} \right) - \frac{K}{R^2} \cdot \left(\frac{\partial u_\theta}{\partial \theta} + u_r \right) \quad (12b)$$

$$+ \frac{b}{R} \cdot N_T - \frac{b}{R^2} \cdot \frac{\partial^2 M_T}{\partial \theta^2} = \rho A \cdot \frac{\partial^2 u_r}{\partial t^2}$$

where N_T and M_T are the thermal force and bending moment acting on the rectangular cross-section of the ring, arising from the temperature variation across the ring width, and are expressed, respectively, as below:

$$N_T = E \cdot \alpha_T \cdot \int_{-b/2}^{b/2} \Delta T \cdot dy \quad (13a)$$

$$M_T = E \cdot \alpha_T \cdot \int_{-b/2}^{b/2} \Delta T \cdot y \cdot dy \quad (13b)$$

where ΔT is the temperature variation from the ambient temperature (T_0), due to thermoelastic coupling. In order to evaluate N_T and M_T explicitly, the temperature variation across the ring width needs to be found.

Strain, temperature, and displacement

Consisting of thermal strain and the strain from normal stress, the total normal strains toward the circumferential, radial, and Z -axis directions, take the following forms, respectively:

$$\varepsilon_{\theta\theta} = \frac{\sigma_{\theta\theta}}{E} + \alpha_T \cdot \Delta T \quad (14a)$$

$$\varepsilon_{rr} = -\nu \cdot \frac{\sigma_{\theta\theta}}{E} + \alpha_T \cdot \Delta T \quad (14b)$$

$$\varepsilon_{zz} = -\nu \cdot \frac{\sigma_{\theta\theta}}{E} + \alpha_T \cdot \Delta T \quad (14c)$$

where ν is the Poisson's ratio.

The normal strains toward the Z -axis and radial directions can be further expressed as:

$$\varepsilon_{zz} = \varepsilon_{rr} = -\nu \cdot \varepsilon_{\theta\theta} + (1 + \nu) \cdot \alpha_T \cdot \Delta T \quad (15)$$

In terms of the radial and circumferential displacements, the normal strain toward the circumferential direction is written as:

$$\varepsilon_{\theta\theta} = \frac{1}{R} \cdot \frac{\partial u_{\theta}}{\partial \theta} + \frac{u_r}{R} + \frac{y}{R^2} \cdot \left[\frac{\partial u_{\theta}}{\partial \theta} - \frac{\partial^2 u_r}{\partial \theta^2} \right] \quad (16)$$

Heat conduction

In the presence of thermoelastic coupling, the governing equation for heat conduction is expressed as below:

$$\chi \cdot \nabla^2 \Delta T - \frac{\partial \Delta T}{\partial t} = \frac{E \cdot \alpha_T \cdot T_0}{\rho \cdot C_p \cdot (1-2\nu)} \cdot \frac{\partial}{\partial t} (\nabla \cdot \bar{u}) \quad (17)$$

where $\nabla \cdot \bar{u}$ is the volume change caused by the vibrations:

$$\nabla \cdot \bar{u} = (1-2\nu) \cdot \varepsilon_{\theta\theta} + 2 \cdot (1+\nu) \cdot \alpha_T \cdot \Delta T \quad (18)$$

Substituting the above volume change into eq. (17) leads to the following relation:

$$\left[1 + 2\Delta_E \cdot \frac{(1+\nu)}{(1-2\nu)} \right] \cdot \frac{\partial \Delta T}{\partial t} = \chi \cdot \frac{\partial^2}{\partial y^2} (\Delta T) - \frac{\Delta_E}{\alpha_T} \cdot \frac{\partial}{\partial t} [\varepsilon_{\theta\theta}] \quad (19)$$

where the temperature variation along the circumferential direction has been neglected.

With the assumption of time-harmonic vibrations, the coupled flexural-mode vibration variables are in the forms:

$$\Delta T = \Theta \cdot e^{j\omega_{nc} t} \quad (20a)$$

$$u_{\theta} = U_{\theta} \cdot e^{j\omega_{nc} t} \quad (20b)$$

$$u_r = U_r \cdot e^{j\omega_{nc} t} \quad (20c)$$

where ω_{cn} is the n th coupled complex frequency, as given by eq. (4). Θ , U_{θ} , and U_r are the amplitudes of the corresponding vibration variables.

Based on eq.s (20), eq. (19) can be rewritten as:

$$\frac{\partial^2 \Theta}{\partial y^2} - \frac{j\omega_{nc}}{\chi} \cdot \Theta = \frac{\Delta_E}{\alpha_T} \cdot \frac{j\omega_{nc}}{\chi} \cdot \left\{ \frac{1}{R} \cdot \frac{\partial U_{\theta}}{\partial \theta} + \frac{U_r}{R} + \frac{y}{R^2} \cdot \left[\frac{\partial U_{\theta}}{\partial \theta} - \frac{\partial^2 U_r}{\partial \theta^2} \right] \right\} \quad (21)$$

The solution to eq. (21) can be expressed as below:

$$\Theta = A \cdot \sin(ky) + B \cdot \cos(ky) - \frac{\Delta_E}{\alpha_T} \cdot \left\{ \frac{1}{R} \cdot \frac{\partial U_{\theta}}{\partial \theta} + \frac{U_r}{R} + \frac{y}{R^2} \cdot \left[\frac{\partial U_{\theta}}{\partial \theta} - \frac{\partial^2 U_r}{\partial \theta^2} \right] \right\} \quad (22)$$

where $k = \sqrt{\omega_{nc} / j\chi}$. Since the first term in the bracket is equal to zero for the flexural-mode vibrations, it will be omitted in the following derivation.

The adiabatic boundary conditions at the inner and outer peripheries of the ring require:

$$\frac{\partial \Theta}{\partial y} \Big|_{\pm b/2} = 0 \quad (23)$$

The substitution of the boundary conditions into the solution (22) gives the temperature variation across the ring width:

$$\Theta \approx -\frac{\Delta_E}{\alpha_T} \cdot \left\{ \frac{1}{R^2} \cdot \left[\frac{\partial U_{\theta}}{\partial \theta} - \frac{\partial^2 U_r}{\partial \theta^2} \right] \right\} \cdot \left[\frac{\sin(ky)}{k \cdot \cos(k \cdot b/2)} - y \right] \quad (24)$$

SOLUTION TO THERMOELASTIC DAMPING

The substitution of the temperature variation (24) into the thermal loads (13) leads to the following expressions:

$$M_T = -\left\{ \frac{24}{k^3 \cdot b^3} \cdot [\tan(k \cdot b/2) - kb/2] - 1 \right\} \cdot \Delta_E \cdot \frac{b^3}{12} \cdot \frac{E}{R^2} \cdot \left[\frac{\partial U_{\theta}}{\partial \theta} - \frac{\partial^2 U_r}{\partial \theta^2} \right] \quad (25a)$$

$$N_T = \frac{E \cdot h}{R} \cdot \Delta_E \cdot \left\{ \frac{\partial U_{\theta}}{\partial \theta} + U_r \right\} \quad (25b)$$

The substitution of the above expressions into eq.s (12) yields the thermoelastic-coupled governing equations for the in-plane flexural-mode vibrations:

$$\rho A \cdot \frac{\partial^2 u_{\theta}}{\partial t^2} = \frac{D}{R^4} \cdot \left[1 + \left\{ 1 + f(\omega_{nc}) \right\} \cdot \Delta_E \right] \cdot \left(\frac{\partial^2 u_{\theta}}{\partial \theta^2} - \frac{\partial^3 u_r}{\partial \theta^3} \right) + (1 - \Delta_E) \cdot \frac{K}{R^2} \cdot \left(\frac{\partial^2 u_{\theta}}{\partial \theta^2} + \frac{\partial u_r}{\partial \theta} \right) \quad (26a)$$

$$\rho A \cdot \frac{\partial^2 u_r}{\partial t^2} = \frac{D}{R} \cdot \left[1 + \left\{ 1 + f(\omega_{nc}) \right\} \cdot \Delta E \right] \cdot \left(\frac{\partial^3 u_\theta}{\partial \theta^3} - \frac{\partial^4 u_r}{\partial \theta^4} \right) - (1 - \Delta E) \cdot \frac{K}{R^2} \cdot \left(\frac{\partial u_\theta}{\partial \theta} + u_r \right) \quad (26b)$$

where the complex function $f(\omega_{nc})$ is given by:

$$f(\omega_{nc}) = \frac{24}{k^3 \cdot b^3} \cdot [kb/2 - \tan(k \cdot b/2)] \quad (27)$$

Summarizing the above derivation, the thermoelastic-coupled governing equations for the flexural-mode vibrations is identical in form to the uncoupled eq.s (6), except that the isothermal value of D is substituted by a frequency-dependent value:

$$D_{\omega_{nc}} = E \cdot \left[1 + \left\{ 1 + f(\omega_{cn}) \right\} \cdot \Delta E \right] \cdot I \quad (28)$$

Hence, incorporating the thermoelastic coupling into eq. (9) gives rise to the following expression for the resonant frequency:

$$\omega_{nc} = \omega_n \cdot \left[1 + \left\{ 1 + f(\omega_n) \right\} \cdot \frac{\Delta E}{2} \right] \quad (29)$$

where ω_n is the n th uncoupled angular resonant frequency and the corrections of order ΔE^2 are neglected.

The above equation consists of the real part and imaginary part. Substituting eq. (27) into the expression for the complex frequency leads to the following relations:

$$Re(\omega_{cn}) = \omega_n \cdot \left(1 + \frac{\Delta E}{2} \left(1 - \frac{6}{\xi^3} \cdot \frac{\sinh(\xi) - \sin(\xi)}{\cosh(\xi) + \cos(\xi)} \right) \right) \quad (30)$$

$$Im(\omega_{cn}) = \omega_n \cdot \frac{\Delta E}{2} \left(\frac{6}{\xi^2} - \frac{6}{\xi^3} \cdot \frac{\sinh(\xi) + \sin(\xi)}{\cosh(\xi) + \cos(\xi)} \right) \quad (31)$$

where $\xi = b \sqrt{\frac{\omega_n}{2\chi}}$ (32)

Equation (30) indicates that the frequency shift from thermoelastic coupling is completely negligible, compared with the frequency mismatch between drive and sense modes, arising from fabrication tolerance.

Using eq. (5), the quality factor of thermoelastic damping (Q_{TED}) in the flexural-mode vibrations of a ring gyroscope is given by:

$$Q_{TED}^{-1} = \frac{E \cdot \alpha_T^2 \cdot T_0}{\rho \cdot C_P} \cdot \left(\frac{6}{\xi^2} - \frac{6}{\xi^3} \cdot \frac{\sinh(\xi) + \sin(\xi)}{\cosh(\xi) + \cos(\xi)} \right) \quad (33)$$

The above exact solution to thermoelastic damping in a ring is identical in form to that of thermoelastic damping in a rectangular beam [8], except that the resonant frequency in eq. (31) is from that of a ring (11). As explained in the literature [8], eq. (32) also predicts a similar Lorentzian behavior with a single thermal relaxation time. When $\xi \ll 1$ (low frequency), the difference between the Wong's work and the exact result (32) is less than 1%. The error from the Wong's work can be more than 10%, when the thermoelastic damping falls into the adiabatic side (high frequency).

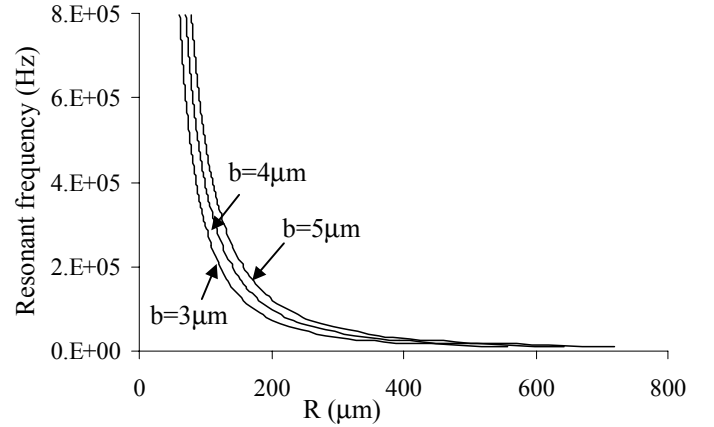
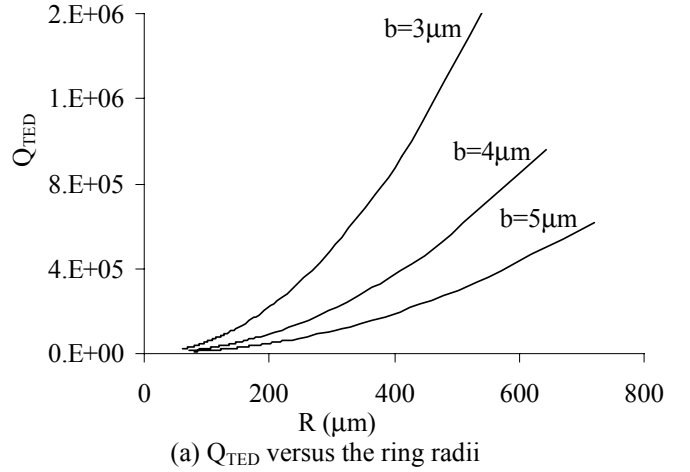


Fig. 4: The characteristics of the Q_{TED} and resonant frequencies of the 2nd flexural-mode versus the ring radii for different ring width

Figure 4 shows the characteristics of Q_{TED} and resonant frequencies of the 2nd flexural mode versus the ring radii for different ring width. It should be noted that the curve in fig. 4(a) falls into the left side of the peak of thermoelastic damping behavior. For the same ring width, the resonant frequency decreases while Q_{TED} increases with the ring radius. It may be explained by the fact that as the ring becomes larger, its thermal

relaxation time decreases. For the same ring radius, the resonant frequency increases while Q_{TED} decreases with the ring width, which is due to the increase of the thermal relaxation time.

Figure 5 shows the characteristics of the Q_{TED} and resonant frequencies versus the ring radii for different flexural modes while the ring width is kept constant. For the same ring width, the resonant frequency increases while the Q_{TED} decreases with the flexural mode orders. Since the thermal relaxation time increases with the flexural mode orders, the increase of Q_{TED} with the mode orders is expected.

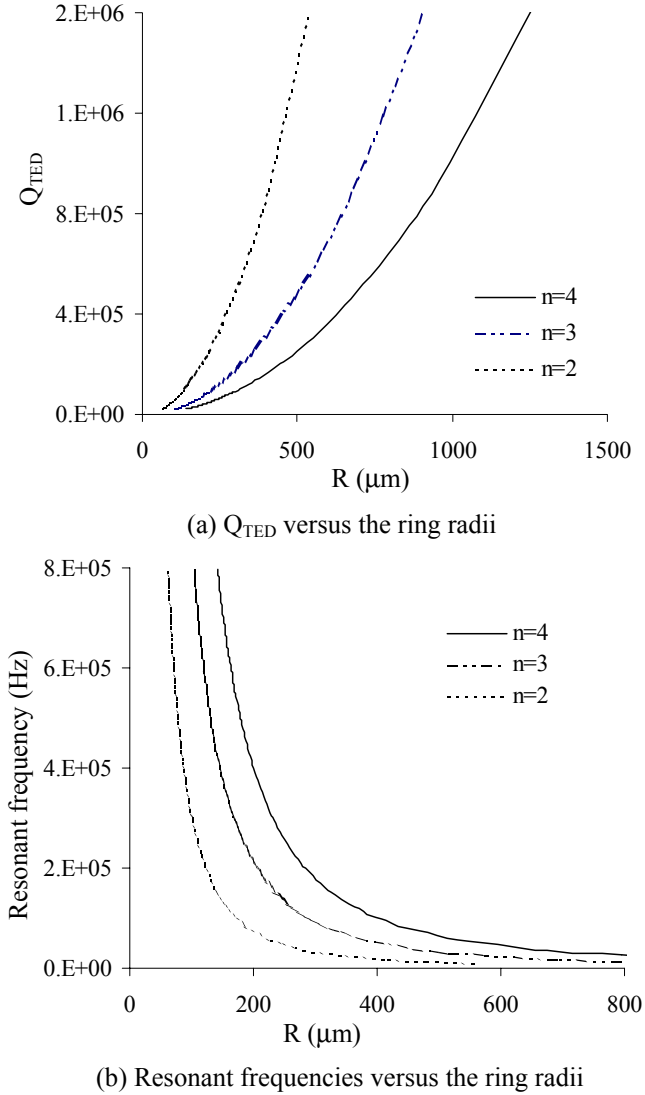


Fig. 5: The characteristics of Q_{TED} and resonant frequencies versus the ring radii for different flexural modes with ring width $b=3\mu\text{m}$

EXPERIMENTAL VERIFICATION

In order to demonstrate its validity, this analytical model is compared with the experimental data. Table 1 lists the measured quality factors (Q_{measured}) [9] and the calculated Q_{TED} of the second flexural-mode of different sizes of ring gyroscopes, demonstrating good agreement. It is clear from this comparison that thermoelastic damping is a significant source of dissipation for micromachined ring gyroscopes. Support loss

is negligible due to the cancellation of the forces from the support beams [13].

ξ	2.694	2.597	1.088	1.154	0.721
Ring radius (mm)	3	3	2	2	2
Ring width (μm)	120	117	50	52	38
Frequency (kHz)	13.8	13.49	12.97	13.49	9.85
Q_{measured}	10,500	10,000	24,000	22,000	48,000
Q_{TED}	10,650	10,390	21,880	19,730	47,690

Table 1: Comparison between measured quality factor and the calculated Q_{TED} of the second-order modes of different sizes of ring gyroscopes.

DISCUSSION

Support loss

For a ring gyroscope operating in vacuum, support loss through the center anchor needs to be addressed. Figure 6 shows a schematic view of forces applied on the center anchor during the flexural-mode vibrations in a ring gyroscope. The flexural-mode vibrations in the ring cause the radial and circumferential displacements at the ring end of the support beams, respectively.

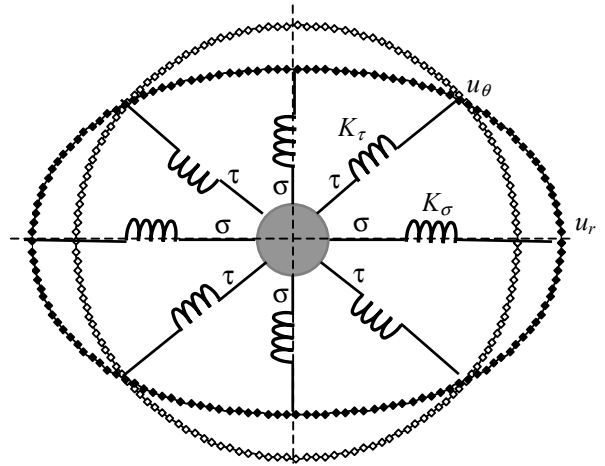


Fig. 6: Schematic view of forces applied on the center anchor during the flexural-mode vibrations in a ring gyroscope

Through the support beams, these radial and circumferential displacements are transferred into the normal and circumferential stresses at the anchor end of the support beams, respectively. Based on the analytical model we have developed previously for disk resonators [11], there are two ways to decrease support loss: 1) reducing the stiffness of the support beams, which means that the forces applied on the anchor is reduced; 2) reducing the anchor size, which means the cancellation between those opposite forces is more complete.

Mechanical noise floor

We have identified that thermoelastic damping is the dominant energy loss mechanism, which is fundamental and always impose an upper limit on the quality factor, while support loss might be alleviated through improved design and fabrication. The mechanical noise floor of a ring gyroscope is evaluated by:

$$\Omega_{mechanical} = \frac{1}{4A_g \cdot q_d} \sqrt{\frac{4k_b \cdot T_0}{\omega_n \cdot M \cdot Q}} \cdot \sqrt{BW} \quad (34)$$

where A_g is the angular gain; q_d is the drive amplitude; k_b is Boltzmann's constant; BW is the bandwidth; M is the equivalent mass of a ring gyroscope, calculated as below:

$$M = \pi \cdot \rho \cdot b \cdot h \cdot R \quad (35)$$

By substituting eq.s (11), (33), and (35) into Equations (34), the fundamental performance limit for the mechanical noise floor in a ring gyroscope can be obtained:

$$\Omega_{mechanical} = \frac{1}{4A_g \cdot q_d \cdot \sqrt[4]{E \cdot \rho}} \sqrt{4k_b \cdot T_0} \cdot \Pi \cdot \sqrt{BW} \quad (36)$$

where Π is the expression related to ring dimensions and flexural-mode orders, expressed as below:

$$\Pi = \sqrt{\frac{1}{\frac{b^2 \cdot h}{R} \cdot Q \cdot \frac{n(n^2 - 1)}{\sqrt{n^2 + 1}}}} \quad (37)$$

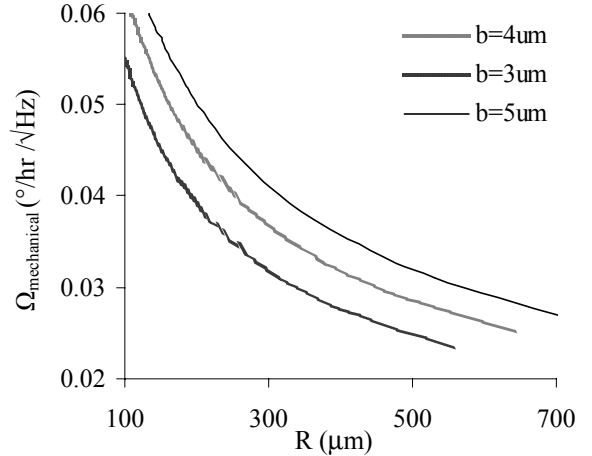
As indicates in eq.s (37), in order to decrease the mechanical noise floor, both the ring thickness and width need to be increased, while the ring radius needs to be decreased. The higher-order modes are preferred for smaller mechanical noise floor.

Figure 7 illustrates the characteristics of the attainable $\Omega_{mechanical}$ and corresponding resonant frequency versus ring radius at different ring width, with ring thickness $10\mu\text{m}$, drive amplitude $1\mu\text{m}$, and temperature 300K . In order to keep the governing equations for the flexural-mode vibrations valid, the ring radius is kept more than $100\mu\text{m}$. As illustrated in fig. 7(a), in order to reduce the mechanical noise floor, the ring width need to be decreased while the ring radius need to be increased. It is worth mentioning that the resonant frequency, shown in fig. 7(b), should be chosen so as not to impose large electronic noise. Depending on the fabrication technology used, the ring thickness can be increased for higher rate-resolution, while the drive amplitude is limited to the linear range of the vibrations.

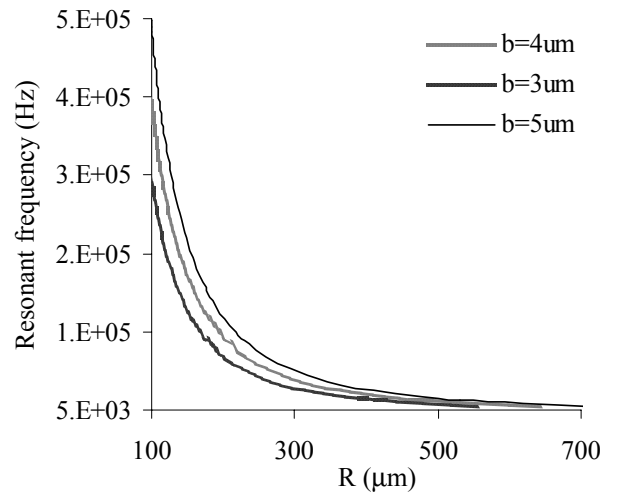
CONCLUSION

Due to significant importance of quality factor in a ring gyroscope, we have derived an exact expression for evaluating the quality factor of thermoelastic damping in the flexural-mode vibrations of a ring gyroscope. It is shown that the maximum thermoelastic damping is associated with environmental temperature and the material properties of the ring, while independent of the flexural mode orders. This damping in a free-edged ring gyroscope exhibits a similar Lorentzian behavior with a single thermal relaxation time as Zener's well-known approximation for a rectangular beam. The validity of this model has been demonstrated through comparison with experimental data. Besides providing significant insight to the geometrical design in high-Q ring gyroscopes, this work also defines the performance limit of a

ring gyroscope, regarding its attainable mechanical noise floor. Further study on support loss in a ring gyroscope will help predict its quality factor more accurately.



(a) Q_{TED} versus the ring radius



(b) Resonant frequency versus ring radius

Fig. 7: The characteristics of $\Omega_{mechanical}$ and corresponding 2nd-order resonant frequency versus ring radius at different ring width ($h=10\mu\text{m}$, $q_d=1\mu\text{m}$, and $T_0=300\text{K}$)

ACKNOWLEDGMENTS

We gratefully acknowledge support from DARPA HERMIT program under contract # W31P4Q-04-1-R001.

REFERENCES

- [1] Michael W. Putty, 1995, "A Micromachined Vibrating Ring gyroscope", Ph. D. Dissertation, University of Michigan.
- [2] Farrokh Ayazi, 2000, "a High Aspect-Ration High-Performance Polysilicon Vibrating Ring gyroscope", Ph. D. Dissertation, University of Michigan.
- [3] Yazdi, N., Ayazi, F., and Najafi, K., 1998, "Micromachined Inertial Sensors", Proceedings of the IEEE, pp. 1640-1659.
- [4] Farrokh Ayazi and Khalil Najafi, 2001, "A HARPSS Polysilicon Vibrating Ring Gyroscope", Journal of Microelectromechanical Systems, pp. 169-179.

- [5] Witold Nowacki, 1975, *Dynamic Problems of Thermoelasticity*, Noordhoff, Leyden.
- [6] Clarence Zener, 1937, "Internal Friction in Solids I. Theory of Internal Friction in Reeds," *Physical Review* **52**, pp.230-235.
- [7] Clarence Zener, 1938, "Internal Friction in Solids II General Theory of Thermoelastic Internal Friction," *Physical Review* **53**, pp. 90-99.
- [8] Ron Lifshitz and M. L. Roukes, 2000, "Thermoelastic Damping in Micro-and Nanomechanical Systems", *Physical Review B*, **61**, pp.5600-5609.
- [9] Wong, S. J., Fox, C. H. J., McWilliam, S., Fell, C. P., and Eley, R., 2004, "A Preliminary Investigation of Thermo-elastic Damping in Silicon Rings," *Journal of Micromechanics and Microengineering*, **14**, pp. 108-113.
- [10] Zhili Hao, Siavash Pourkamali, and Farrokh Ayazi, 2004, "VHF Single Crystal Silicon Elliptic Bulk-mode Capacitive Disk Resonators Part I: Design and Modeling", *Journal of Microelectromechanical Systems*, **13**, No. 6, pp. 1043-1053.
- [11] Werner Soedel, 1993, *Vibrations of Shells and Plates*, Marcel Dekker, Second Edition.
- [12] Zhili Hao, Ahmet Erbil, and Farrokh Ayazi, 2003, "An Analytical Model for Support Loss in Micromachined Beam Resonators with In-plane Flexural Vibrations," *Sensors and Actuators A*, **109**, pp.156-164.
- [13] Zhili Hao and Farrokh Ayazi, 2005, "Support Loss in Micromechanical Disk Resonators," the 18th IEEE International Conference on Micro Electro Mechanical Systems (MEMS 2005), Miami, pp. 137-141.